COMPLEX CRATER FORMATION BY OBLIQUE IMPACTS ON THE EARTH AND MOON. T. M. Davison and G. S. Collins. Impacts and Astromaterials Research Centre, Department of Earth Science and Engineering, Imperial College London, London, SW7 2AZ, United Kingdom (E-mail: thomas.davison@imperial.ac.uk).

Introduction: Impact crater populations on planetary surfaces can reveal a large amount of information about the bombardment history of the planet. However, to decode these cratering records and extract detail of the impacting population and the surface age of the planet requires a method to convert the impact parameters (size, velocity, angle, etc.) and target properties (strength, gravity, density) to a crater size and shape, known as crater scaling. While recent progress has improved our understanding of crater scaling for small, simple craters and the largest (>300-km) impact basins, impactor-to-crater scaling of mid-sized, so-called "complex" craters, 10-300 km in diameter is less well constrained.

Numerical simulations of crater formation are used to bridge the gap between observations of existing craters and laboratory scale impact experiments. Most previous numerical models of complex crater formation have assumed a vertical incidence angle (to allow the simulations to be run more expediently in 2D). However, the most likely impact angle is 45°, and 90% of all impacts occur at angles $<70°$ from the target plane. When studies have simulated oblique impacts they have often used a reduced impact speed to mitigate the additional computational expense of a fully 3D calculation [e.g., 1]. In this work, we simulate complex crater formation in 3D to constrain the effects of impact angle and velocity on crater scaling and to provide insight into kinematic differences in crater collapse following an oblique impact.

Modeling: We simulated oblique incidence impact events using the iSALE3D shock physics code [1–4]. The target was composed of a 33 km thick granitic crust overlying a dunite mantle. Both materials used an ANEOS-derived tabular equation of state [5, 6]. The acoustic fluidization "block model" was used to allow late-stage collapse of the transient crater [7]. Two sets of simulations were performed; one with Earth's gravity, and one with the Moon's gravity. Impactors had diameters (L) of 6, 9 and 14 km, and impact angles (θ) of 30, 40, 45, 50, 60, 75 and 90°. Impact velocity (v) was varied between 10 and 30 km s^{-1} on Earth, and 5 and 30 km s^{-1} on the Moon. The impacts produced transient craters with diameters in the range 40–100 km on Earth and 60–100 km on the Moon. Final craters ranged in diameter from 60–160 km on Earth and 70–200 km on the Moon. All models had a resolution of 14 cppr (cells per projectile radius), resulting in cells sizes of 222.2, 320 and 500 m for the three different impactor sizes.

Transient crater diameters at the pre-impact level were calculated at the time of maximum crater volume. A typical simulation is shown in Fig. 1, for L = 14 km, v = 20 km s^{-1} and θ = 45° on Earth. The crater reaches its maximum depth at t = 20 s, (Fig. 1a), its maximum volume at t = 65 s (Fig. 1b) and by 500 s, modification has ended and the crater has reached its final morphology (Fig. 1c). Since the along-range and cross-range diameters of the craters can be quite different in oblique cases, here we use the diameter of a circle with the equivalent area of the crater planform at the pre-impact elevation to allow comparisons between models (termed the "equivalent radius"). Final crater measurements were taken after all material in the simulation had ceased moving.

Oblique impact crater scaling: Well-established π-group crater scaling for large craters relates the scaled

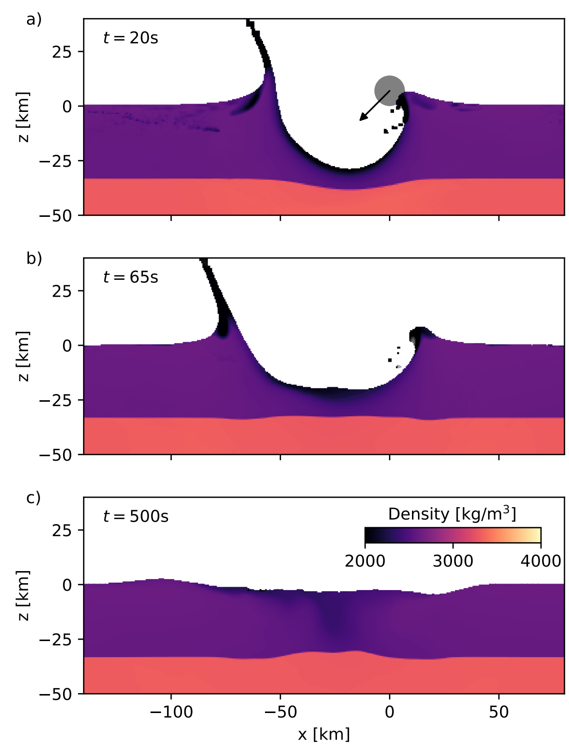

Figure 1: Snapshots from a simulation of a 14 km diameter impactor with a velocity of 20 km s^{-1} and an impact angle of 45° on Earth. The three frames show the crater at its (a) maximum depth (b) maximum volume and (c) final morphology. The grey circle in (a) shows the size and location of the impactor at the point of impact, and the arrow shows its trajectory.

transient crater diameter ($\pi_D = D_{tr}(\rho/m)^{1/3}$) or volume ($\pi_V = \rho V_{tr}/m$) to the gravity-scaled size ($\pi_2 = gL/v^2$), where ρ is the target density, m is the impactor mass, D_{tr} is the transient diameter, V_{tr} is the transient volume and g is the surface gravity. For vertical impacts these relationships can be expressed as power laws:

$$\pi_D = C_D \pi_2^{-\beta}, \quad \pi_V = C_V \pi_2^{-\gamma} \tag{1}$$

where C_D, C_V, β and γ are constants [e.g., 8].

To extend Eq. 1 to oblique impacts, an often-used assumption is to replace the impact velocity with the vertical component of the impact velocity. In this case, the gravity-scaled size becomes $\pi_2 = gL/(v \sin\theta)^2$. In the scaling relationship often used for large-scale cratering, $\beta = 0.22$ and $\gamma = 0.65$ [8], and thus according to this assumption, transient crater diameter would scale with $\sin^{0.44}(\theta)$, and transient crater volume with $\sin^{1.3}(\theta)$. However, our simulations suggest that the dependence of crater diameter on impact angle is much weaker, and that transient diameter instead scales between approximately $\sin^{0.05}(\theta)$ and $\sin^{0.25}(\theta)$ and the transient volume scales between $\sin^{0.60}(\theta)$ and $\sin^{1.1}(\theta)$ (see grey shaded regions in Fig. 2). This is similar to the dependence found in previous models of relatively low-speed oblique impacts [1].

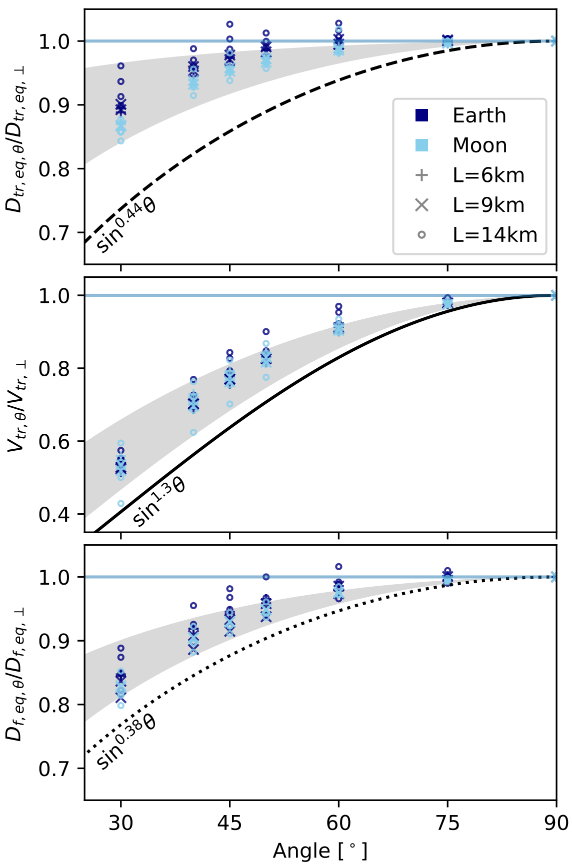

Figure 2: Dependence on impact angle of (a) transient crater diameter, (b) transient crater volume and (c) final crater diameter. Dark blue symbols represent impacts on Earth, and light blue symbols represent impacts on the Moon. Grey shaded regions highlight the approximate range that fits the data; see details in text.

Final crater scaling: Final crater diameters (measured at the pre-impact surface elevation) were approximately 1.5–1.7 times larger than the transient craters on Earth, and 1.2–1.4 times larger than the transient craters on the Moon; these are in good agreement with the scaling from [9, 10]. A recent modified complex crater scaling relationship [11] predicted that final crater diameter should scale with $\sin^{0.38}(\theta)$. In Fig 2(c), our simulations again show a weaker dependence on impact angle; the shaded grey region shows most simulations exhibit final crater scaling in the range $\sin^{0.15}(\theta)$ to $\sin^{0.30}(\theta)$.

Conclusions: We have simulated complex crater formation on Earth for a range of impact angles and velocities. Our simulations show that craters formed by oblique incidence impacts are typically larger than predicted by existing scaling relationships. Our extensive dataset of oblique impact complex crater simulations also contains a wealth of morphometric and structural information that can be used to better characterise the influence of impact angle and speed on crater and ejecta asymmetry.

Acknowledgements: We thank the developers of iSALE (isale-code.de), in particular Dirk Elbeshausen. TMD and GSC acknowledge support from STFC grant ST/S000615/1. This work was performed using the DiRAC Data Intensive service at Leicester, operated by the University of Leicester IT Services, which forms part of the STFC DiRAC HPC Facility (www.dirac.ac.uk). The equipment was funded by BEIS capital funding via STFC capital grants ST/K000373/1 and ST/R002363/1 and STFC DiRAC Operations grant ST/R001014/1. DiRAC is part of the National e-Infrastructure.

References: [1] Elbeshausen, D. et al. (2009). *Icarus*, 204:716–731. [2] Collins, G. S. et al. (2016). iSALE-Dellen Manual. DOI: 10.6084/m9.figshare.3473690. [3] Elbeshausen, D. & Wünnemann, K. (2011). *Proc. 11th HVIS*, 287–301. [4] Amsden, A. A. & Ruppel, H. M. (1981). *LANL Report*, LA-8905:151p. [5] Pierazzo, E. et al. (1997). *Icarus*, 127:408–423. [6] Benz, W. et al. (1989). *Icarus*, 81:113–131. [7] Wünnemann, K. & Ivanov, B. A. (2003). *Planet. Space Sci.* 51:831–845. [8] Schmidt, R. M. & Housen, K. R. (1987). *Int. J. of Impact Eng.* 5:543–560. [9] McKinnon, W. B. & Schenk, P. M. (1985). *LPSC XVI*, 544–545. [10] Collins, G. S. et al. (2005). *Meteorit. Planet. Sci.* 40:817–840. [11] Johnson, B. C. et al. (2016). *Icarus*, 271:350–359.